Acta Universitatis Sapientiae
Electrical and Mechanical Engineering, 16 (2024) 26–37

DOI: 10.47745/auseme-2024-0003

Numerical Analysis of Efficiency Improvement in Flat Plate Solar Collectors using Offset Strip Fins

Mohamed Chakib MALTI[1], Zakaria SARI HASSOUN[1], Khaled ALIANE[1], Younes REKIOUK[3], Bastien DI PIERRO[2], Mohammed Abdelbassit KHERRAFI[3]

[1] MECACOMP Laboratory, Mechanical Engineering Department, Faculty of Technology, Abou Bekr Belkaid University, Tlemcen, Algeria
[2] Fluid Mechanics and Acoustics Laboratory, Claude Bernard University, Lyon 1, UMR 5509, Lyon; France
[3] ETAP Laboratory, Mechanical Engineering Department, Faculty of Technology, Abou Bekr Belkaid University, Tlemcen, Algeria

Manuscript received October 15, 2024; revised November 06, 2024

Abstract: This study aims to enhance the efficiency of flat plate solar collectors by integrating offset strip fins and utilizing Ansys Fluent for numerical analysis, validating results from a SolidWorks-designed solar air dryer. It outlines system components and objectives based on a standard model, supporting both theoretical and experimental analyses for applications in air conditioning and agro-food drying. Key boundary conditions, such as inlet temperature, air velocity, and absorber emissivity, were defined while maintaining experimental dimensions. Mesh tests ensured simulation accuracy for essential thermodynamic parameters, including outlet temperature and pressure, using the realizable *k-epsilon* turbulence model. The advanced model features obstacles that increase the heat transfer area by 53.6 % and create secondary turbulent flow. Staggered offset strip fins improved temperature by 12.6 % at an air velocity of 0.92 m/s (*Re* = 6000), significantly enhancing the overall effectiveness of the solar collector.

Keywords: Flat plate solar collectors, offset strip fins, temperature, velocity.

1. Introduction

The swift advancement of industrialization and rising energy demands strain limited fossil fuel resources and the environment. Therefore, it is essential to investigate all avenues for renewable energy generation. Among renewable sources, solar energy presents significant potential for fulfilling energy requirements sustainably. Consequently, various technologies have been developed and are being enhanced to utilize this potential effectively [1]. The

sun provides the most plentiful and accessible energy on Earth through direct solar irradiance and indirect forms like wind and hydro. Hence, solar energy stands as a viable, eco-friendly alternative that is readily available and can satisfy both present and future global energy needs without adverse effects [2]. Solar collectors are crucial for efficiently capturing Earth's abundant solar energy [3], with flat plate air collectors frequently employed for low to medium temperature applications due to their simplicity and ease of maintenance. Nonetheless, their relatively low efficiency poses challenges in justifying the initial costs over extended periods [4]. This paper emphasizes recent research efforts aimed at enhancing the efficiency of flat plate air collectors through design optimization, addressing the dual challenge of maximizing solar energy absorption at minimal cost while ensuring energy availability at night [5].

2. Technics of increasing the performance of a flat air solar collector

A flat plate air collector captures solar radiation for fluid heating using a dark absorber sheet that converts solar energy into heat, which is then transferred to circulating fluid. The absorber sheets, made from metals like copper or aluminum, are coated for better absorption, while integrated pipes carry the fluid. Glazing, typically glass or plastic, allows solar radiation in while minimizing heat loss, with insulation materials used to further reduce losses [6-9]. Experimental investigation by A. E. Kabeel et al [10] about thermal performance of flat and V-corrugated plate solar air heaters with and without Phase Change Materials as thermal energy storage, the authors integrated paraffin to the solar collectors for optimizing the global yield, they finally concluded that The V-corrugated solar air heater with PCM maintains outlet temperatures 1.5–7.2 °C higher than ambient for 3.5 hours after sunset at a flow rate of 0.062 kg/s, compared to 1–5.5 °C for the flat plate heater over 2.5 hours. At a lower flow rate of 0.009 kg/s, the V-corrugated heater stays 2–13 °C above ambient for 7.5 hours, while the flat plate heater remains 1.5–10 °C higher for 6 hours. M. A. Kherrafi et al [11] studied an indirect solar dryer, concluding it enhanced economic efficiency and reduced greenhouse gas emissions [12]. Furthermore H. Alsammarraie et al [13] explored nanofluid characteristics and their effects on heat transfer, identifying key factors like particle size and concentration. M. Nejlaoui et al [14] optimized flat plate solar collector performance in Qassim, achieving higher efficiency with a smaller collector area. Vednath P. Kalbande et al [15] reviewed nanofluid-based solar collectors integrated with thermal energy storage, noting that nanofluid properties significantly enhance system performance. P. Visconti et al [16] found that Al2O3-based nanofluids improved traditional solar thermal collector efficiency. Finally, Kamel Haine and Dagnija Blumberga [17] evaluated solar energy

efficiency across continents, emphasizing the importance of technical and social factors in enhancing solar energy efficiency.

3. Materials and methods

3.1 Solar panel

The convective heat exchange in a covered solar collector, involving the glass pane, absorber surface, and external environment, is illustrated in *Fig. 1a.* Additionally, *Fig. 1b* depicts the heat fluxes and thermal losses associated with a flat-plate solar collector [18].

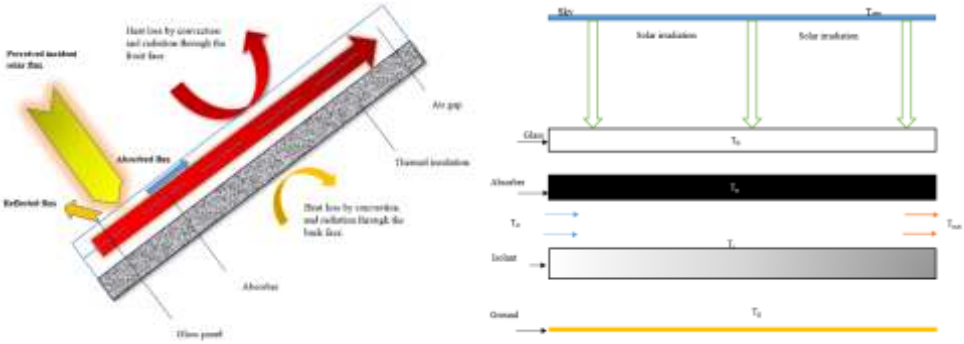

(1a) *(1b)*

Figure 1: Different heat exchanges and most important components in a flat plate solar collector

3.2 Modeling equations of fluid flow

The system model is governed by averaged equations (1), (2) and (3) [19-21]:

$$\frac{\partial U_i}{\partial x_i} = 0\,, \tag{1}$$

$$\frac{\partial U_i}{\partial t} + U_j \cdot \frac{\partial U_i}{\partial x_j} = -\frac{1}{\rho} \cdot \frac{\partial P}{\partial x_i} + \frac{\mu}{\rho} \cdot \frac{\partial^2 U_i}{\partial x_i{}^2}\,, \tag{2}$$

$$\frac{\partial T}{\partial t} + U_j \cdot \frac{\partial T}{\partial X_J} = \frac{\partial}{\partial x_j}\left[\left(\frac{\mu}{Pr} + \frac{\mu_t}{Pr_t}\right) \cdot \frac{\partial T}{\partial x_j}\right] + \frac{1}{\rho \cdot C_p} \cdot \varphi\,, \tag{3}$$

where the unknown U_i is the velocity field (m·s^{-1}), P is the pressure (Pa), and T is the temperature (K). The physical parameters are ρ which is the density

($kg \cdot m^{-3}$), μ represents the dynamic viscosity ($Pa \cdot s^{-1}$), and C_p the specific heat capacity ($J \cdot kg^{-1} \cdot K^{-1}$).

The equation (1) represents the conservation of mass for an incompressible fluid, the equation (2) describes conservation of momentum, and equation (3) illustrates energy conservation.

4. Validation and results discussion

4.1 Physical model

The boundary conditions that have been defined are as follows: Inlet temperature T_{in} = 300 K, inlet velocity $V_{in} = V_i$, $i = 1…5$, thermal flux Q = 800 W/m², dark aluminum absorber emissivity is 0,9. Simulation parameters are gathered in the *Table 1*.

Table 1: Air properties

Air properties	ρ ($Kg.m^{-3}$)	μ ($kg \cdot m^{-1} \cdot s^{-1}$)	λ ($W \cdot m^{-1} \cdot K^{-1}$)	*Pr*
Value	1,225	0,00001789	0,0242	0,744

On one hand the Nusselt number can be calculated by Petukhov formula [22]:

$$Nu_p = \frac{(f/8)\cdot(Re-1000)\cdot Pr}{1+12.7\cdot(f/8)^{\frac{1}{2}}\cdot(Pr^{\frac{2}{3}}-1)}, \quad (4)$$

$$f = (0{,}79 \cdot \ln(Re) - 1.64)^{-2}, \quad (5)$$

$$Re = \frac{V \cdot D_h}{\nu}. \quad (6)$$

The equation (4) is valid when: $0{,}5 < Pr < 2000$ and $3000 < Re < 5\times10^6$ [22].

Equation (5) and (6) illustrate the friction factor and the Reynolds number respectively.

From another part, the theoretical equation of Nusselt number is defined by:

$$Nu_D = \frac{h \cdot D_h}{k}. \quad (7)$$

h is known to be the heat transfer coefficient ($W \cdot m^{-2} \cdot K^{-1}$), D_h is the hydraulic diameter (m), k is the thermal conductivity ($W \cdot m^{-1} \cdot K^{-1}$), V is the air velocity ($m \cdot s^{-1}$) and ν is the kinematic viscosity ($m \cdot s^{-2}$), and *Pr* is the Prandtl number (dimensionless). *Fig. 2* and *Fig. 3* describe the isometric and top views of the collector's section, while Table 2 provides the length, width and thickness of

this one. The hydraulic diameter for a rectangular duct is defined by a specific formula that is shown in equation (8) [23,24]**:**

$$D_h = \frac{4 \cdot l \cdot h}{2 \cdot (l+h)}, \tag{8}$$

where *l* is the width (m), and *h* is the thickness (m).

Table 2: Solar collector dimensions

Dimensions	*L*	*l*	*h*	D_h
Value (mm)	2000	1000	50	95

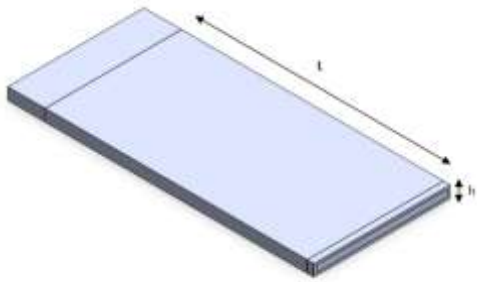

Figure 2: Top view of the solar collector

Figure 3: Isometric view of the solar collector

In order to stabilize the fluid flow and obtain a compatible pressure value in the interesting area, also to be able to calculate the performance coefficient (*PEC*), a calming section of up to three times the length of the hydraulic diameter (D_h) has been made at the entrance of the solar collector. Whereas a length almost equal to half of the hydraulic diameter has been established at the

outlet of the collector to make sure that the fluid interacts only with the obstacles as well as the wall of the flat plate solar collector.

4.2 Mesh

The mesh was selected based on the number of elements, skewness, and orthogonal quality to ensure accurate numerical results. *Fig. 4* illustrates the mesh structure applied to the collector's geometry.

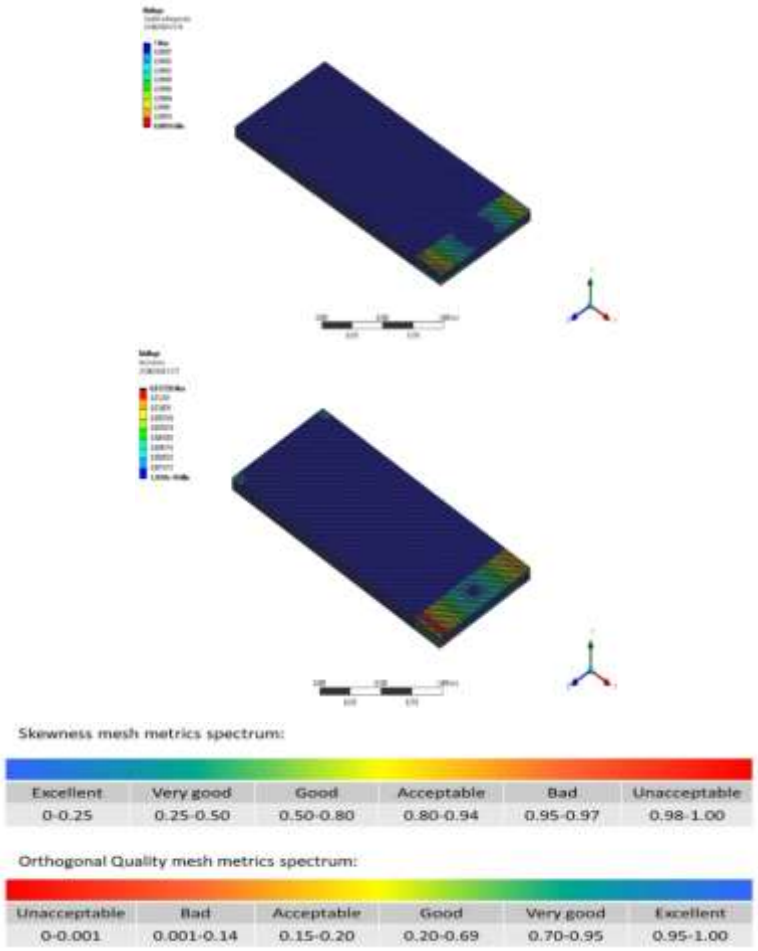

Figure 4: Orthogonal and skewness mesh quality scale

To demonstrate that the results are independent of the mesh used, various meshes were created and presented in Table 3 and *Fig. 4*. The parameters

monitored included the air temperature at the solar collector's outlet and the pressure in the (*zx*) plane, with the air velocity maintained at 0.61 m/s (*Re* = 4000).

Table 3: Outlet temperature and pressure variation as function of number of elements

Meshes	1	2	3	4
Size of the elements	0.01	0.006	0.005	0.004
Number of elements	223088	1035358	1767860	3570060
T_{out} (K)	307.2428	307.0313	306.9700	306.8016
Temperature relative error (%)		0.0688	0.01996	0.0548
Pressure (Pa)	0.1131	0.1068	0.1051	0.1006
Pressure relative error (%)		5.5702	1.5917	4.2816

The graph indicates that the temperature and pressure remain nearly constant across different element counts. The relative errors listed in Table 3 are negligible, leading to the selection of the smallest number of elements for the numerical study due to its quick calculation and accurate results.

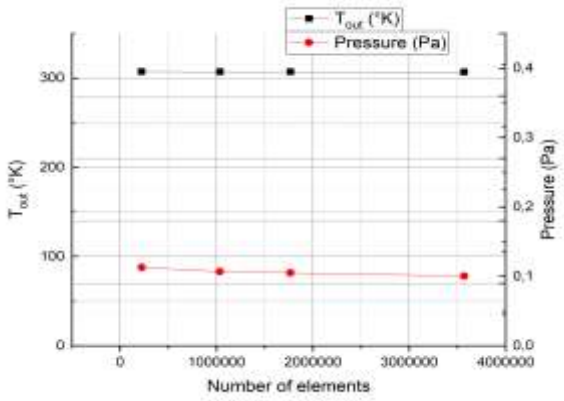

Figure 5: Outlet temperature variation as function of the size of elements used

Numerical validation involves varying air inlet velocity, calculating the Nusselt number using the Petukhov correlation (4) [25], and comparing it with simulation results for model validation (6), as shown in *Table 4* and *Figure 5*.

Table 4: Variation of Nu_D and Nu_P as function of Reynolds number

V_{in} (m/s)	0.92	1.23	1.54	1.85	2.15
Reynolds number	6000	8000	10000	12000	14000
h (W/m².K)	5.61	6.65	7.54	8.44	9.11
Nu_D (6)	22.02	26.10	29.60	33.73	35.76
Nu_P (4)	20.06	25.60	30.72	35.52	40.28
Relative error (%)	9.77	1.95	3.65	6.72	11.22

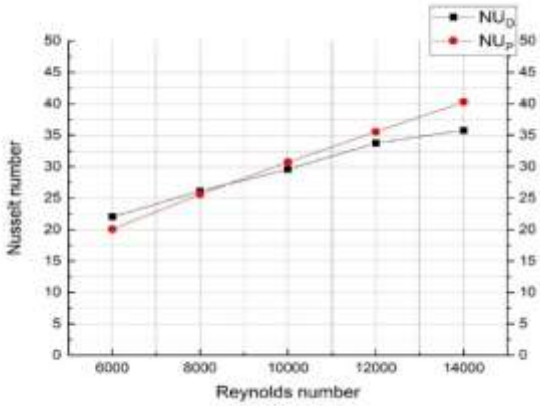

Figure 6: Variation of the Nusselt numbers as function of Reynolds number

The graph shows that the Nusselt number (Nu_D) varies proportionally with the Reynolds number (Nu_P) between 6000 and 14000. The model is validated for Reynolds numbers 7000 to 12000, with low relative errors (1.95% to 6.72%). However, it is unreliable outside this range, showing errors over 9% at Re = 6000 and over 11% at Re = 14000.

5. Personal contribution and efficiency enhancement

To enhance solar air collector efficiency, 10 rows of 12 staggered metallic offset strip fins were added, increasing the heat transfer area by 53.6%. *Fig. 7* illustrates the dimensions of these aluminum obstacles.

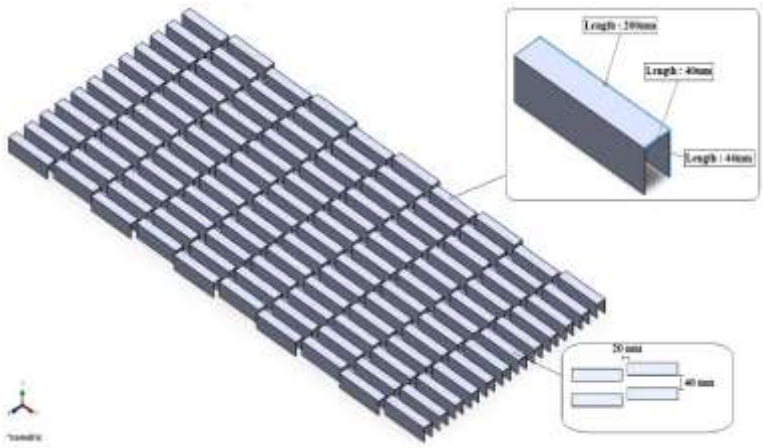

Figure 7: Isometric view of the offset strip fins

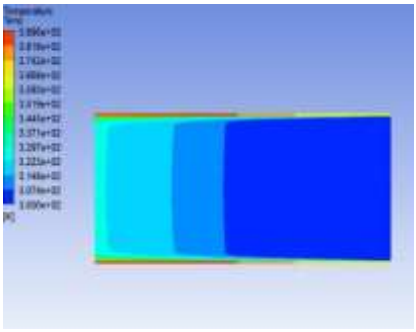

Figure 8: Temperature's contour in offset strip fins solar collector

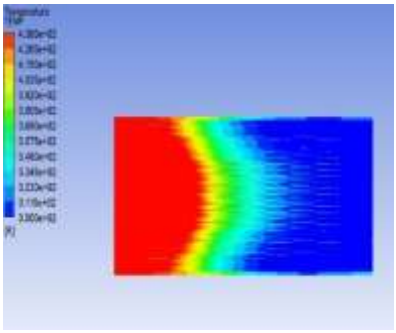

Figure 9: Temperature's contour in smooth solar collector

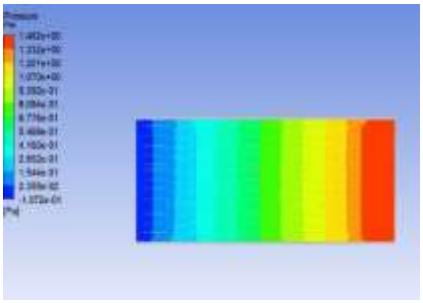

Figure 10: Pressure's contour in offset strip fins solar collector

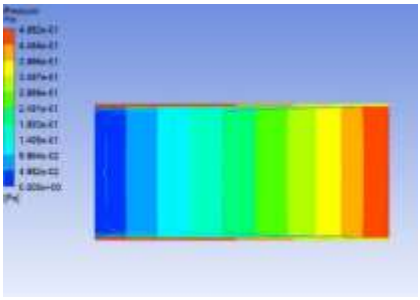

Figure 11: Pressure's contour in smooth solar collector

Fig. 8 and *Fig. 9* show temperature contours for offset strip fins (OSF) and smooth solar collectors respectively, at T_{in} = 300 K, Q = 900 W/m², and V_{in} = 0.92 m/s (Re = 6000). The fluid flow goes from left to right. The maximum temperature of the smooth collector reaches 389 K, while the maximum temperature of the OSF model reaches 438 K, improving thermal efficiency by 12.6 %. *Fig. 10* and *Fig. 11* indicate that adding strip fins causes significant pressure drops – 0.496 Pa to 0 Pa for the smooth collector and 1.462 Pa to -0.107 Pa for the OSF – due to increased friction force. This analysis helps calculate the performance coefficient (*PEC*), confirming the OSF model's thermal and geometric validity.

The performance coefficient formula is represented by [26]:

$$PEC = \frac{Nu/Nu_s}{(f/f_s)^{\frac{1}{3}}}, \tag{7}$$

where the index *s* refers to the smooth surface, *Nu* and *f* are Nusselt and friction factor, respectively [27].

$$f = \frac{\Delta P}{\frac{L}{D_h}\cdot\frac{\rho V^2}{2}}. \tag{8}$$

Table 5. below gathered inlet and outlet air pressures to evaluate the *PEC* number at an inlet velocity of 0.92 m·s^{-1} (Re = 6000).

Table 5: Inlet and outlet pressures in both OSF and simple solar collectors

Collector type	Required parameters	P_{in} (Pa)	P_{out} (Pa)	Friction factor	Nusselt Number
OSF solar collector		1.93	0.85	0.035	51.88
Smooth solar collector		0.56	0.029	0.017	29.32
PEC		1.39			

General conclusion

This research involved a 3D numerical comparative analysis of a smooth solar air collector and one with offset strip fins (OSF). It began with an introduction to global energy demand and an overview of solar collectors, discussing their components, recent studies, and mathematical models. The analysis highlighted the advantages and disadvantages of thermal solar collectors, we then highlighted the simple model validation, and suggested a brand-new model by adding offset strip fins increasing heat transfer area by 53.6 %, which systematically led to enhance the collector's efficiency. The findings concluded that integrating obstacles into a simple solar air collector

enhances its yield, reaching a performance coefficient of 1.39 for a Reynolds number of 6000, and a maximum temperature increase of approximately 12.6 %, demonstrating the superiority of the improved model, suitable for various applications, both industrial and domestic.

Acknowledgments

The support from Abou Bekr Belkaid University, Tlemcen, is fully acknowledged for giving me the original versions of the software used for this study.

References

[1] Suman S., Khan M. K., and Pathak M., "Performance enhancement of solar collectors-A review", Renewable and Sustainable Energy Reviews. vol. 49 pp. 192–210, Sept. 2015.

[2] Chen Z., Furbo S., Perers B., Fan J., and Andersen E., "Efficiencies of flat plate solar collectors at different flow rates", Energy Procedía, vol. 30, pp. 65–72, 2012.

[3] Chopra K., Tyagi V. V., Pandey A. K., and Sari A., "Global advancement on experimental and thermal analysis of evacuated tube collector with and without heat pipe systems and possible applications", Applied Energy, vol. 228, pp. 351–389, 2018.

[4] Sabiha M. A., Saidur R., Mekhilef S., and Mahian O., "Progress and latest developments of evacuated tube solar collectors", Renewable and Sustainable Energy Reviews, vol. 51, pp. 1038–1054, 2015.

[5] Tang R., Sun Z., Li Z., Yu Y., Zhong H., and Xia C., "Experimental investigation on thermal performance of flat plate collectors at night", Energy Conversion and Management, vol. 49, pp. 2642–2646, 2008.

[6] Pandey K. M., and Chaurasiya R., "Review on analysis and development of solar flat plate collector", Renewable and Sustainable Energy Reviews, vol. 67, pp. 641–650, 2017.

[7] Nguyen M. H., Ouldboukhitine S. E., Durif S., Saulnier V., and Bouchair A., "Passive fire protection of steel profiles using wood", Engineering Structures, vol. 275, pp. 2023, Mar. 2022, https://doi.org/10.1016/j.engstruct.2022.115274.

[8] Abuṣka M., Kayapunar A., "Experimental and numerical investigation of thermal performance in solar air heater with conical surface", Heat and Mass Transfer, vol. 57, pp. 1791–1806, Apr. 2021.

[9] Khoukhi M., Maruyama S., "Theoretical approach of a flat plate solar collector with clear and low-iron glass covers taking into account the spectral absorption and emission within glass covers layer", Renewable Energy, vol. 30, pp. 1177–1194, 2005.

[10] Kabeel A. E. et al., "Experimental investigation of thermal performance of flat and v-corrugated plate solar air heaters with and without PCM as thermal energy storage", Energy Conversion and Management, 2016.

[11] Hamed M. et al., "Numerical analysis of an integrated storage solar heater", International Journal of Hydrogen Energy, 2017.

[12] Kherrafi M. A. et al., "Performance enhancement of indirect solar dryer with offset strip fins: Experimental investigation and comparative analysis", Solar Energy, 2023.

[13] Alsammarraie H. et al., "Numerical and experimental studies of the nanofluid characteristics that affect heat transfer enhancement: Review and comparison", Journal of Advanced Research in Fluid Mechanics and Thermal Sciences, Aug. 2023.
[14] Nejlaoui M., Alghafis A., Sadig H., "Design optimization and experimental validation of low-cost flat plate collector under central Qassim climate", Journal of Applied and Computational Mechanics, vol. 7, no. 2, 2021.
[15] Kalbande V. P., "Advancements in thermal energy storage systems by applications of nanofluid-based solar collectors: A review", Environmental and Climate Technologies, vol. 24, no. 1, pp. 310–340, 2020, https://doi.org/10.2478/rtuect-2020-0018.
[16] Visconti P. et al., "Measurement and control system for thermosolar plant and performance comparison between traditional and nanofluid solar thermal collectors", International Journal on Smart Sensing and Intelligent Systems, vol. 9, no. 3, Sept. 2016.
[17] Haine K., Blumberga D., "Evaluation of solar energy efficiency by composite index over four continents", Environmental and Climate Technologies, vol. 25, no. 1, pp. 774–785, 2021, https://doi.org/10.2478/rtuect-2021-0058.
[18] Houhou H., "Theoretical and experimental study of solar drying of certain agro-food products", Memoir of Magister in Mechanical Engineering, University of Biskra, pp. 9–35, 39.
[19] Taler D., "Numerical modelling and experimental testing of heat exchangers", Springer International Publishing, Cham, 21 May 2018.
[20] Alfatih A. et al., "On the formulation of mass, momentum, and energy conservation in the KdV equation", Acta Applicandae Mathematicae, vol. 133, pp. 113–131, 2014.
[21] Bekkouche S., "Modeling the thermal behavior of some solar devices", Doctoral thesis, Abou-bakr-Belkaid University – Tlemcen, 2008.
[22] Taler D. et al., "Simple heat transfer correlations for turbulent tube flow", E3S Web of Conferences, vol. 13, p. 0200, 2017.
[23] Karma R., "Thermo-hydraulic performance of solar air heater with finned absorber plate forming multiple rectangular air flow passages in parallel under laminar flow conditions", Applied Thermal Engineering, vol. 221, pp. 119673, Feb. 2023.
[24] Curd E. F. et al., "Air-handling processes", Industrial Ventilation Design Guidebook, pp. 677–806, 2001.
[25] Sleicher C. A., Rouse M. W., "A convenient correlation for heat transfer to constant and variable property fluids in turbulent pipe flow", International Journal of Heat and Mass Transfer, vol. 18, no. 5, pp. 677–683, May 1975.
[26] Li X. L. et al., "A performance recovery coefficient for thermal-hydraulic evaluation of recuperator in supercritical carbon dioxide Brayton cycle", Energy Conversion and Management, vol. 256, p. 115393, Mar. 2022.
[27] Ramadhan A. I. et al., "Experimental and numerical study of heat transfer and friction factor of plain tube with hybrid nanofluids", Case Studies in Thermal Engineering, vol. 22, p. 100782, Dec. 2020.